Quantum Criticality of Two-Dimensional Quantum Magnets with Long-Range Interactions

Sebastian Fey, Sebastian C. Kapfer, and Kai Phillip Schmidt
Lehrstuhl für Theoretische Physik I, Staudtstraße 7, Universität Erlangen-Nürnberg, D-91058 Erlangen, Germany

(Received 19 February 2018; published 4 January 2019)

We study the critical breakdown of two-dimensional quantum magnets in the presence of algebraically decaying long-range interactions by investigating the transverse-field Ising model on the square and triangular lattice. This is achieved technically by combining perturbative continuous unitary transformations with classical Monte Carlo simulations to extract high-order series for the one-particle excitations in the high-field quantum paramagnet. We find that the unfrustrated systems change from mean-field to nearest-neighbor universality with continuously varying critical exponents. In the frustrated case on the square lattice the system remains in the universality class of the nearest-neighbor model independent of the long-range nature of the interaction, while we argue that the quantum criticality for the triangular lattice is terminated by a first-order phase transition line.

DOI: 10.1103/PhysRevLett.122.017203

The understanding of quantum phase transitions at zero temperature has been an active research field over many decades, since the diverging quantum fluctuations of quantum many-body systems at a quantum-critical point lead to intriguing universal behavior giving rise to many fascinating quantum materials with novel collective effects. The physical properties close to a zero-temperature quantum-critical point can be classified for most systems by universality classes, which only depend on the dimension and the symmetry of the underlying system. As a consequence, the critical behavior of many physical systems can be described by paradigmatic models for each universality class, which in many cases correspond to interacting spin systems [1].

One of the most important microscopic models is the ferromagnetic transverse-field Ising model (TFIM). This unfrustrated system realizes a quantum phase transition between a quantum paramagnet and a $\mathcal{Z}_2$-symmetry-broken phase for any lattice in any dimension d [2,3]. The corresponding universality class is the one of the classical Ising model in dimension $d+1$ [2–4]. In general, the quantum-critical properties of unfrustrated models with short-range interactions are well understood. The situation becomes more interesting in the presence of frustration where different types of quantum-critical behavior as well as exotic states of quantum matter are known to occur. Important examples in the framework of fully frustrated TFIMs are the antiferromagnetic TFIM on the triangular and pyrochlore lattice [5–7]. For the triangular TFIM, an order by disorder mechanism gives rise to a ground state where translational symmetry is broken and the universality class of the quantum phase transition is 3D XY [5,8–10]. In contrast, on the pyrochlore lattice, disorder by disorder leads to a quantum-disordered Coulomb phase in the antiferromagnetic TFIM [11–13] displaying emergent quantum electrodynamics, and the quantum phase transition to the high-field quantum paramagnet is first order [14].

All of the above systems are restricted to short-range interactions. However, there are many important physical systems where long-range interactions are relevant [15–27]. Important examples are dipolar interactions between spins in spin-ice materials giving rise to emergent magnetic monopoles [18], effective long-range magnetic interactions between zigzag edges in graphene [28], as well as trapped cold-ion systems in quantum optics for which the nature of interactions can be varied flexibly and which have realized the long-range TFIM (LRTFIM) on the triangular lattice [22,23,27].

The critical behavior of quantum systems with long-range interactions is much less understood. Several studies have focused on the TFIM chain with long-range interactions [29–33]. For a ferromagnetic Ising exchange there are three different regimes. Besides 2D-Ising criticality, as for the nearest-neighbor TFIM chain, and mean-field (MF) behavior, for intermediate long-range interactions, there is a window with continuously varying critical exponents. In contrast, a recent investigation of the frustrated antiferromagnetic TFIM chain with long-range interactions indicates that the critical behavior is always 2D Ising independent of the nature of the long-range interaction [32]. Much less is known in $2+1$ dimensions [34], since numerical investigations are much harder to perform. This is especially true when it comes to the interplay of long-range interactions and frustration. In this Letter, we combine high-order series expansions with classical Monte Carlo simulations to investigate such interesting and challenging quantum systems.

Model.—We study the LRTFIM given by

$$\mathcal{H} = -\frac{1}{2}\sum_{\mathbf{j}}\sigma^z_{\mathbf{j}} - \frac{\lambda}{2}\sum_{\mathbf{i}\neq\mathbf{j}}\frac{1}{|\mathbf{i}-\mathbf{j}|^{\alpha}}\sigma^x_{\mathbf{i}}\sigma^x_{\mathbf{j}}, \tag{1}$$

with Pauli matrices $\sigma_{\mathbf{i}}^{x/z}$ describing spins-1/2 located on lattice sites $\mathbf{i}$. Positive (negative) λ correspond to (anti) ferromagnetic interactions. Tuning the positive parameter α changes the long-range behavior of the interaction, where $\alpha = \infty$ recovers the nearest-neighbor TFIM. In this work we focus on the square and triangular lattice illustrated in Fig. 1.

Approach.—We perform high-order series expansions in λ about the high-field limit with the long-range Ising interactions acting as a perturbation to

$$\mathcal{H}_0 = -\frac{1}{2}\sum_{\mathbf{j}} \sigma_{\mathbf{j}}^z. \tag{2}$$

The ground state of $\mathcal{H}_0$ is given by $|\uparrow\uparrow\cdots\uparrow\rangle$ while the lowest excitations are single local spin flips. To obtain a quasiparticle (QP) description we perform a Matsubara-Matsuda transformation $\sigma_{\mathbf{j}}^x = \hat{b}_{\mathbf{j}}^\dagger + \hat{b}_{\mathbf{j}}$ and $\sigma_{\mathbf{j}}^z = 1\text{–}2\hat{n}_{\mathbf{j}}$ [35]. Here, $\hat{b}_{\mathbf{j}}^{(\dagger)}$ are hard-core boson annihilation (creation) operators and $\hat{n}_{\mathbf{j}} \equiv \hat{b}_{\mathbf{j}}^\dagger \hat{b}_{\mathbf{j}}$ counts the number of particles on site $\mathbf{j}$. This gives Eq. (1) in a QP language,

$$\mathcal{H} = \sum_{\mathbf{j}} \hat{n}_{\mathbf{j}} - \frac{\lambda}{2}\sum_{\mathbf{i}\neq\mathbf{j}} \frac{1}{|\mathbf{i}-\mathbf{j}|^\alpha}(\hat{b}_{\mathbf{i}}^\dagger \hat{b}_{\mathbf{j}}^\dagger + \hat{b}_{\mathbf{i}}^\dagger \hat{b}_{\mathbf{j}} + \text{H.c.}), \tag{3}$$

up to a constant of $-N/2$.

Next we apply perturbative continuous unitary transformations (PCUTs) [36] using white graphs [37] to transform Eq. (1), order by order in λ, to an effective QP-conserving Hamiltonian $\mathcal{H}_{\text{eff}}$, as it has been done successfully for the one-dimensional LRTFIM [31]. As a consequence, $\mathcal{H}_{\text{eff}}$ is block diagonal in the QP number $\hat{Q} \equiv \sum_{\mathbf{i}} \hat{n}_{\mathbf{i}}$ and the quantum many-body system is mapped to an effective few-body problem. Here we consider the one-QP block which can be expressed as

$$\mathcal{H}_{\text{eff}}^{1\text{QP}} = E_0 + \sum_{\mathbf{i},\boldsymbol{\delta}} a_{\boldsymbol{\delta}} (\hat{b}_{\mathbf{i}}^\dagger \hat{b}_{\mathbf{i}+\boldsymbol{\delta}} + \text{H.c.}), \tag{4}$$

with the ground-state energy E_0 and the hopping amplitudes $a_{\boldsymbol{\delta}}$. The one-QP Hamiltonian Eq. (4) is diagonalized by Fourier transformation yielding $\mathcal{H}_{\text{eff}}^{1\text{QP}} = E_0 + \sum_{\mathbf{k}} \omega(\mathbf{k}) \hat{b}_{\mathbf{k}}^\dagger \hat{b}_{\mathbf{k}}$. Although we calculated $\omega(\mathbf{k})$ at various $\mathbf{k}$ [38], in the following, we focus on the one-QP gap Δ, which is the minimum of the one-QP dispersion $\omega(\mathbf{k}) = a_{\mathbf{0}} + \sum_{\boldsymbol{\delta}\neq\mathbf{0}} a_\delta \cos(\mathbf{k}\cdot\boldsymbol{\delta})$. The gap is located at $\mathbf{k} = \mathbf{0}$ in the ferromagnetic cases and at $\mathbf{k} = (\pi,\pi)$ [$\mathbf{k} = \pm(2\pi/3, -2\pi/3)$] for the antiferromagnetic LRTFIM on the square [triangular] lattice in the α ranges we have studied (see Fig. 1 for the definition of basis vectors).

The PCUT determines the hopping amplitudes $a_{\boldsymbol{\delta}}$ and therefore the one-QP dispersion $\omega(\mathbf{k})$ as a high-order series expansion in λ in the thermodynamic limit. This can be done most efficiently via a full graph decomposition in linked graphs $\mathcal{G}$ exploiting the linked-cluster theorem [37]. While for Hamiltonians with short-range interactions the main challenge lies in the generation of and calculation on linked graphs contributing in a given order, for long-range interactions the difficulty is shifted to the final embedding [31]. In order k perturbation theory, all linked graphs with up to k links may contribute in the calculation. The embedding of the graph-specific contribution $a_{\boldsymbol{\delta}}^{\mathcal{G}}$ to the hopping amplitudes $a_{\boldsymbol{\delta}}$ in Eq. (4) in the infinite lattice requires the embedding of every single link infinitely many times due to the long-range character of the interaction. As a result of the infinite number of possible embeddings on the lattice for each graph, a conventional linked-cluster expansion becomes problematic. At this point white graphs are essential [37], since they allow us to extract the generic linked contributions from graphs in a first step while the embedding on a specific lattice is done only at the end of the calculation. Here we perform the PCUT on each graph by introducing different couplings $\lambda_j^{\mathcal{G}}$ with $j \in \{1,\ldots,n\}$ on the n links of $\mathcal{G}$. The resulting linked contributions in terms of the $\lambda_j^{\mathcal{G}}$ are then embedded in the infinite system by identifying the sites of graph $\mathcal{G}$ with the sites of the lattice and therefore replacing $\lambda_j^{\mathcal{G}}$ with the true interactions $\lambda|\mathbf{i}-\mathbf{j}|^{-\alpha}$ for each pair of sites $\mathbf{i}$ and $\mathbf{j}$ on the lattice. An exemplary embedding is given in the Supplemental Material [38]. In general, the embedding procedure leads to the occurrence of nested infinite sums. In the most complex nested sum in order k there are dk infinite sums, where d is the dimension of the lattice. Here we calculated series expansions of order 9 for Δ, which results in 18 nested sums for the most difficult terms. In total, a number of 1068 different graphs have to be treated for each $\mathbf{k}$ and α. Let us stress that these calculations are tremendously more demanding compared to those in the one-dimensional LRTFIM where a brute-force evaluation of the nested sums up to order 8 is still feasible [31]. In two dimensions, an analogue calculation would only reach order 4, which is certainly not sufficient to extract quantum-critical properties of the LRTFIM. Substantial progress is therefore needed to reach order 9, which we achieved by implementing classical Markov-chain Monte Carlo (MCMC) integration techniques. The infinitely large configuration space of embeddings is sampled in order to calculate the coefficients c_k of the gap series $\Delta = \sum_{k=1}^{9} c_k \lambda^k$. Details on the implementation and the performance of the MCMC calculations are given in the Supplemental Material, which

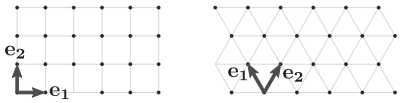

FIG. 1. Illustration of the square (left) and triangular (right) lattice with basis vectors $\mathbf{e_1}$ and $\mathbf{e_2}$.

includes results for the long-range TFIM chain showing the improved quality of our approach even for the one-dimensional case [38]. For a given lattice, exponent α, and momentum $\mathbf{k}$, we sort the resulting nested sums of all graphs in a given perturbative order by the number of sites $N_{\mathcal{G}}$ of the graphs. Then a separate MCMC calculation is performed for each $N_{\mathcal{G}}$ in every order from 1 to 9. Effectively, the problem is reduced to the computation of the classical partition function of an $N_{\mathcal{G}}$-mer with many-body interactions with respect to a linear molecule. Joining all contributions from the various MCMC calculations, we obtain numerical estimates for the coefficients c_k which are given in Ref. [38]. The relative errors of these coefficients are similar for both lattices, but slightly larger for the antiferromagnetic cases. Most importantly, the numerical uncertainty is small enough in the c_k so that any conclusion drawn below is not affected.

The final series of the gap have to be extrapolated in order to extract quantum-critical properties of the LRTFIM. As for the one-dimensional LRTFIM [31], we expect second-order quantum phase transitions out of the high-field quantum paramagnet so that the one-particle gap Δ closes as $(\lambda - \lambda_c)^{z\nu}$ near the quantum-critical point λ_c. Here, z is the dynamical and ν the correlation-length critical exponent. The quantities λ_c and $z\nu$ are then estimated by dlogPadé extrapolation of the gap series. As error bars for these quantities we use the standard deviation of non-defective dlogPadé extrapolants. Further details of the extrapolation and our error estimates are given in Ref. [38].

Results.—We apply our approach to the LRTFIM on the square and triangular lattice, both for a ferromagnetic and an antiferromagnetic Ising exchange. The main goal is to determine the quantum phase diagram and to analyze the universality classes as a function of α.

Ferromagnetic interaction.—In this case the LRTFIM is in the 3D-Ising universality class for $\alpha \to \infty$ on both lattices with a critical exponent $z\nu \approx 0.63$ [47]. As a function of α, a similar behavior as for the 1D LRTFIM is expected [31,48], where the critical exponent $z\nu$ varies continuously in a certain range of α from 2D Ising to the MF value $z\nu = 0.5$. However, the boundaries in α of continuously varying exponents are shifted to $\alpha = 10/3$ and $\alpha = 6$ [48]. In Fig. 2, we show our results for λ_c and $z\nu$ for both lattices (green and blue squares and triangles). We also display MF results as in Refs. [34,38] (dot-dashed lines) and the quantum Monte Carlo data point for $\alpha = 3$ on the triangular lattice (red triangles) [34], which agrees well with our data. For a large $\alpha = 10$ the critical value λ_c is already very close to its nearest-neighbor correspondent. Strengthening the longer-range couplings by reducing α stabilizes the $\mathcal{Z}_2$-broken phase and λ_c decreases. In the limit $\alpha \to 2$ the phase transition happens at $\lambda_c \to 0$, while for exactly $\alpha = 2$ the sums diverge and Eq. (1) becomes ill defined. However, we stress that our results agree with MF calculations (dot-dashed lines in Fig. 2) even in the regime

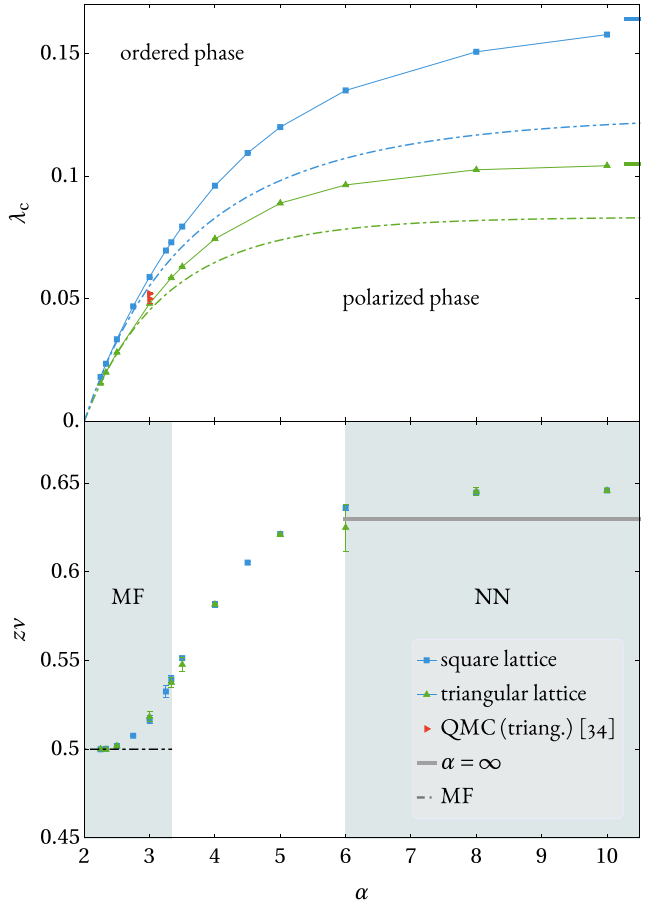

FIG. 2. Critical point λ_c (upper panel) and exponent $z\nu$ (lower panel) are shown as squares (triangles) for the ferromagnetic LRTFIM on the square (triangular) lattice. Error bars represent the standard deviation of nondefective dlogPadé extrapolants. Shaded areas correspond to MF (left) and nearest-neighbor (NN) (right) universality, which are known exactly in these α ranges [48]. Upper panel: Thick lines indicate the quantum-critical points $\lambda_c = 0.16421$ [49] (square lattice) and $\lambda_c = 0.105$ [50] (triangular lattice) for the nearest-neighbor TFIM. MF results are given as dot-dashed lines and the quantum Monte Carlo data as red triangles (see Ref. [34]). Lower panel: The upper (lower) dashed (dot-dashed) line refers to $z\nu \approx 0.63$ [47] ($z\nu = 0.5$) of the nearest-neighbor TFIM (in MF).

$\alpha \leq 2.5$, where the MF ansatz is expected to be quantitatively correct.

Next we discuss the behavior of $z\nu$. It is known that the dlogPadé extrapolation slightly overestimates critical exponents, since it ignores subleading corrections to the critical behavior. As a consequence, for both lattices, the estimate $z\nu \approx 0.65$ for large α is about 3% too large compared to the known value $z\nu \approx 0.63$ [47] of the nearest-neighbor TFIM [47,51]. In the opposite limit of small α, the critical exponent $z\nu$ approaches the MF value 0.5 confirming the expected MF limit. In between we find an interesting continuous variation of $z\nu$ from the MF value to that of the 3D-Ising universality class. Note that we attribute the deviations from 0.5, which is exactly known to be correct

for $\alpha \leq 10/3$ [48], to limitations of the extrapolation which neglects the subleading multiplicative logarithmic correction p at $\alpha = 10/3$ (for a definition of p, see Ref. [38]). Indeed, when extracting p for $\alpha = 10/3$ from the dlogPadé extrapolation by fixing λ_c and $z\nu = 1/2$ as for the one-dimensional LRTFIM [31], we find $p = -0.17(4)$ [$p = -0.143(7)$] for the square [triangular] lattice. These values are remarkably close to $p = -1/6$, which is the prediction for the 3D TFIM from perturbative renormalization group and series expansions [52–56]. The quantum-critical behavior induced by the long-range Ising interaction can therefore effectively be understood in terms of the nearest-neighbor TFIM in an effective spatial dimension. Furthermore, we stress that the estimated critical exponents agree extremely well on both lattices. This property can be seen as a kind of metauniversality because the universality class of both models changes identically with the parameter α.

Antiferromagnetic interaction.—Here we expect an inherently different behavior not only with respect to the ferromagnetic case but also when comparing both lattices. Already in the nearest-neighbor limit $\alpha \to \infty$ one finds two different universality classes, since the TFIM on the triangular lattice displays 3D-XY universality due to the strong geometric frustration resulting in a $\sqrt{3} \times \sqrt{3}$ order at small fields [9,10]. On the square lattice, the long-range Ising interaction introduces again frustration which is, however, expected to be weaker. For both lattices there is no MF limit for small values of α and it is therefore not at all obvious how the quantum-critical behavior changes as a function of α in these frustrated systems.

Our results for λ_c and $z\nu$ are shown for both lattices in Fig. 3. As expected, stronger competing interactions introduced by decreasing α stabilize the quantum paramagnet. We observe that the MCMC approach becomes less reliable for α close to 2 for both lattices [38]. Furthermore, small α values lead to alternating series in $|\lambda|$ with extremely large coefficients c_k which are hard to extrapolate (see also Ref. [38]). This results in rather large error bars for $\alpha \leq 3$, as can be seen in Fig. 3. Consequently, we only show results for $\alpha \geq 2.5$ [58].

As outlined above, limitations in the extrapolation lead to a slightly overestimated $z\nu$ for large α [10,51]. Decreasing α, $z\nu$ stays almost constant and close to the value of the nearest-neighbor TFIM for the investigated α regime. However, the physics at smaller α is likely different on both lattices. On the square lattice, we expect always the same quantum phase transition between the polarized and the Néel ordered state in the full range of α in a similar fashion as deduced for the LRTFIM chain [32] due to the following reasons. We do not find tendencies for a softening of other one-QP modes at different $\mathbf{k}$ [38], which points against a second-order quantum phase transition to a differently ordered state. The critical lines of a variational calculation covering the polarized and the Néel phase [38] is in better agreement with the corresponding PCUT

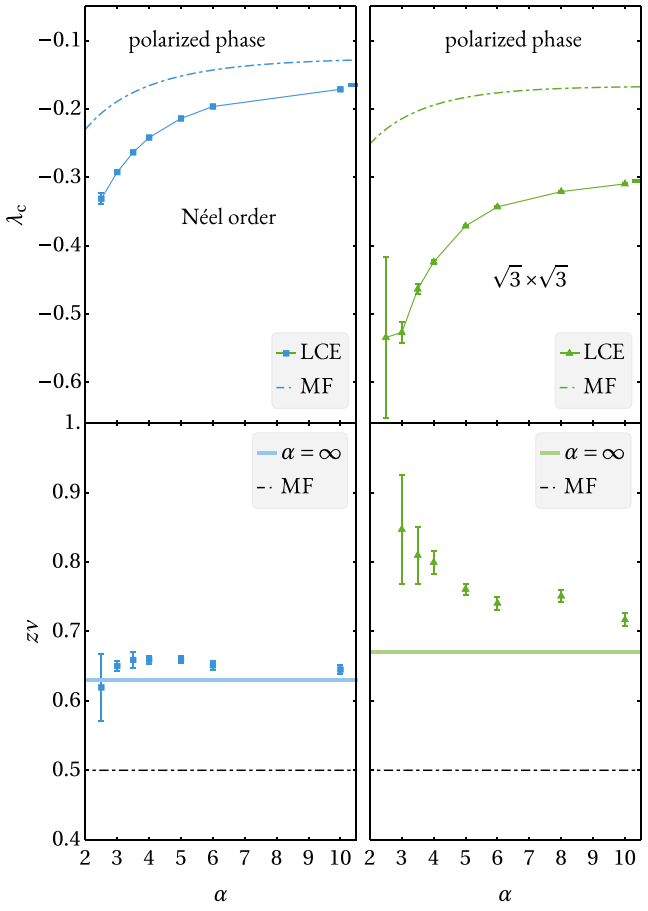

FIG. 3. Critical point λ_c (upper panel) and exponent $z\nu$ (lower panel) are shown as squares (triangles) for the antiferromagnetic LRTFIM on the square (triangular) lattice. Error bars indicate the standard deviation of nondefective dlogPadé extrapolants. Upper panel: Thick lines correspond to $\lambda_c = -0.16421(1)$ [49] ($\lambda_c = -0.305$ [9,10]) for the TFIM on the square (triangular) lattice. Dot-dashed lines show MF results for the transition between the polarized and Néel (left) and $\sqrt{3} \times \sqrt{3}$ (right) order. Lower panel: Thick lines refer to the 3D-Ising exponent $z\nu \approx 0.63$ [47] (left) and 3D-XY exponent $z\nu \approx 0.67$ [57] (right). The dot-dashed line refers to the MF exponent $z\nu = 0.5$.

findings in the whole α range compared to the triangular LRTFIM (see dot-dashed curves in Fig. 3). Finally, we expect the pure long-range Ising model to be Néel ordered for all $\alpha > 0$. Our approach for the square lattice is therefore dominantly limited by the increasing relative error of the MCMC approach for $\alpha \lesssim 2.5$ [38]. On the triangular lattice, in addition, the extrapolation becomes problematic in the same α regime and we expect a different physical scenario. Again, no indication for a gap closing at a different $\mathbf{k}$ is observed [38]. Most likely, the phase transition becomes first order and a stripe-ordered state [38] is realized at small fields for $\alpha \lesssim 2.5$. Indeed, tensor network calculations of the LRTFIM on cylinders find a zigzag-stripe order for $\alpha \lesssim 2.4$ [43] and the full 2D-Ising model displays *straight-stripe* order [39,40].

Most importantly, the phase transition between the straight-stripe order and the polarized phase is known to be first order [39,41]. Consequently, our approach for the triangular lattice is primarily limited by the first-order nature of the phase transition for $\alpha \lesssim 2.5$, which cannot be tracked by investigating gap closings.

Conclusions.—We investigated the largely unexplored interplay of long-range interactions, quantum fluctuations, and frustration in 2D quantum magnets directly in the thermodynamic limit. This was achieved by a technical breakthrough combining high-order series expansions with classical MCMC calculations. The most challenging regime is small α for the frustrated LRTFIMs. It would therefore be desirable to further improve our approach by applying other techniques to extrapolate the series [42,59] and by developing optimized setups for the MCMC technique. Combining our results with similar linked cluster expansions inside the ordered phases could further help to locate first-order phase transitions which we expect for the triangular LRTFIM. Our approach works directly in the thermodynamic limit and it does, *a priori*, not suffer from a sign problem. It can therefore be applied to a large class of interesting systems with long-range interactions in the future allowing the calculation of other physical quantities like correlation functions or bound states between quasiparticles.

We gratefully acknowledge the computational resources and support provided by the HPC group of the Erlangen Regional Computing Center (RRZE).

Note added.—Recently, we became aware of the numerical work by Saadatmand *et al.* [43] who studied the antiferromagnetic triangular lattice LRTFIM on infinitely long cylinders.

[1] S. Sachdev, *Quantum Phase Transitions*, 2nd ed. (Cambridge University Press, Cambridge, England, 2011).
[2] R. Elliott, P. Pfeuty, and C. Wood, Phys. Rev. Lett. **25**, 443 (1970).
[3] P. Pfeuty, J. Phys. C **9**, 3993 (1976).
[4] M. Suzuki, Prog. Theor. Phys. **56**, 1454 (1976).
[5] R. Moessner and S. L. Sondhi, Phys. Rev. B **63**, 224401 (2001).
[6] R. Moessner, Can. J. Phys. **79**, 1283 (2001).
[7] R. Liebmann, in *Statistical Mechanics of Periodic Frustrated Ising Systems*, edited by H. Araki, J. Ehlers, K. Hepp, R. Kippenhahn, H. A. Weidenmüller, and J. Zittartz, Lecture Notes in Physics Vol. 251 (Springer, Berlin, 1986).
[8] D. Blankschtein, M. Ma, A. N. Berker, G. S. Grest, and C. M. Soukoulis, Phys. Rev. B **29**, 5250 (1984).
[9] S. V. Isakov and R. Moessner, Phys. Rev. B **68**, 104409 (2003).
[10] M. Powalski, K. Coester, R. Moessner, and K. P. Schmidt, Phys. Rev. B **87**, 054404 (2013).
[11] L. Balents, Nature (London) **464**, 199 (2010).
[12] M. Hermele, M. P. A. Fisher, and L. Balents, Phys. Rev. B **69**, 064404 (2004).
[13] N. Shannon, O. Sikora, F. Pollmann, K. Penc, and P. Fulde, Phys. Rev. Lett. **108**, 067204 (2012).
[14] J. Röchner, L. Balents, and K. P. Schmidt, Phys. Rev. B **94**, 201111 (2016).
[15] D. Bitko, T. F. Rosenbaum, and G. Aeppli, Phys. Rev. Lett. **77**, 940 (1996).
[16] P. B. Chakraborty, P. Henelius, H. Kjønsberg, A. W. Sandvik, and S. M. Girvin, Phys. Rev. B **70**, 144411 (2004).
[17] S. T. Bramwell and M. J. P. Gingras, Science **294**, 1495 (2001).
[18] C. Castelnovo, R. Moessner, and S. L. Sondhi, Nature (London) **451**, 42 (2008).
[19] E. Mengotti, L. Heyderman, A. Bisig, A. Fraile Rodríguez, L. Le Guyader, F. Nolting, and H. Braun, J. Appl. Phys. **105**, 113113 (2009).
[20] T. Lahaye, C. Menotti, L. Santos, M. Lewenstein, and T. Pfau, Rep. Prog. Phys. **72**, 126401 (2009).
[21] D. Peter, S. Müller, S. Wessel, and H. P. Büchler, Phys. Rev. Lett. **109**, 025303 (2012).
[22] J. W. Britton, B. C. Sawyer, A. C. Keith, C.-C. J. Wang, J. K. Freericks, H. Uys, M. J. Biercuk, and J. J. Bollinger, Nature (London) **484**, 489 (2012).
[23] R. Islam, C. Senko, W. Campbell, S. Korenblit, J. Smith, A. Lee, E. Edwards, C.-C. Wang, J. Freericks, and C. Monroe, Science **340**, 583 (2013).
[24] P. Jurcevic, B. P. Lanyon, P. Hauke, C. Hempel, P. Zoller, R. Blatt, and C. F. Roos, Nature (London) **511**, 202 (2014).
[25] P. Richerme, Z.-X. Gong, A. Lee, C. Senko, J. Smith, M. Foss-Feig, S. Michalakis, A. V. Gorshkov, and C. Monroe, Nature (London) **511**, 198 (2014).
[26] S. Mahmoudian, L. Rademaker, A. Ralko, S. Fratini, and V. Dobrosavljević, Phys. Rev. Lett. **115**, 025701 (2015).
[27] J. G. Bohnet, B. C. Sawyer, J. W. Britton, M. L. Wall, A. M. Rey, M. Foss-Feig, and J. J. Bollinger, Science **352**, 1297 (2016).
[28] C. Koop and S. Wessel, Phys. Rev. B **96**, 165114 (2017).
[29] T. Koffel, M. Lewenstein, and L. Tagliacozzo, Phys. Rev. Lett. **109**, 267203 (2012).
[30] M. Knap, A. Kantian, T. Giamarchi, I. Bloch, M. D. Lukin, and E. Demler, Phys. Rev. Lett. **111**, 147205 (2013).
[31] S. Fey and K. P. Schmidt, Phys. Rev. B **94**, 075156 (2016).
[32] G. Sun, Phys. Rev. A **96**, 043621 (2017).
[33] T. Horita, H. Suwa, and S. Todo, Phys. Rev. E **95**, 012143 (2017).
[34] S. Humeniuk, Phys. Rev. B **93**, 104412 (2016).
[35] T. Matsubara and H. Matsuda, Prog. Theor. Phys. **16**, 569 (1956).
[36] C. Knetter and G. S. Uhrig, Eur. Phys. J. B **13**, 209 (2000).
[37] K. Coester and K. P. Schmidt, Phys. Rev. E **92**, 022118 (2015).
[38] See Supplemental Material at http://link.aps.org/supplemental/10.1103/PhysRevLett.122.017203 for details on the graph embedding, the used Monte Carlo simulations to evaluate the nested infinite sum, tables of the series coefficients of all gap series, a description of the extrapolation scheme applied to the gap series, results for the long-range TFIM chain, the variational and mean-field calculation, and the one-QP dispersion, which includes Refs. [29–31, 34,39–46].
[39] A. Smerald, S. Korshunov, and F. Mila, Phys. Rev. Lett. **116**, 197201 (2016).

[40] J. Koziol, S. Fey, and K. Schmidt (to be published).
[41] S. E. Korshunov, Phys. Rev. B **72**, 144417 (2005).
[42] A. C. Guttmann, in *Phase Transitions and Critical Phenomena*, edited by C. Domb and J. Lebowitz (Academic Press, New York, 1989), Vol. 13.
[43] S. N. Saadatmand, S. D. Bartlett, and I. P. McCulloch, Phys. Rev. B **97**, 155116 (2018).
[44] W. Krauth, *Statistical Mechanics: Algorithms and Computations* (Oxford University Press, Oxford, 2006), Vol. 13.
[45] W. K. Hastings, Biometrika **57**, 97 (1970).
[46] J. M. Borwein, *Lattice Sums Then and Now* (Cambridge University Press, Cambridge, England, 2013), Vol. 150.
[47] F. Kos, D. Poland, D. Simmons-Duffin, and A. Vichi, J. High Energy Phys. 08 (2016) 36.
[48] A. Dutta and J. K. Bhattacharjee, Phys. Rev. B **64**, 184106 (2001).
[49] C. Hamer, J. Phys. A **33**, 6683 (2000).
[50] A. Yanase, J. Phys. Soc. Jpn. **42**, 1816 (1977).
[51] J. Oitmaa, C. Hamer, and Z. Weihong, J. Phys. A **24**, 2863 (1991).
[52] A. Larkin and D. Khmel'Nitskii, Sov. Phys. JETP **29**, 1123 (1969).
[53] E. Brezin, J. C. Le Guillou, and J. Zinn-Justin, Phys. Rev. D **8**, 2418 (1973).
[54] F. J. Wegner and E. K. Riedel, Phys. Rev. B **7**, 248 (1973).
[55] Z. Weihong, J. Oitmaa, and C. Hamer, J. Phys. A **27**, 5425 (1994).
[56] K. Coester, D. G. Joshi, M. Vojta, and K. P. Schmidt, Phys. Rev. B **94**, 125109 (2016).
[57] A. P. Gottlob and M. Hasenbusch, J. Stat. Phys. **77**, 919 (1994).
[58] Note that the critical point for $\alpha = 3$ from quantum Monte Carlo simulations [34] lies above our results. However, this data point has been produced by a data collapse assuming MF exponents, which we think is not appropriate with respect to our findings.
[59] W. Wu, M. Ferrero, A. Georges, and E. Kozik, Phys. Rev. B **96**, 041105 (2017).